Comparison of Electron Paramagnetic Resonance Line Shapes and Electron Spin Relaxation Rates for C_{60}^- and C_{60}^{3-} in 4:1 Toluene:Acetonitrile and Dimethyl Sulfoxide

Sandra S. Eaton,* Andrew Kee, Rachel Konda, and Gareth R. Eaton

Department of Chemistry, University of Denver, Denver, Colorado 80208

Paul C. Trulove[†] and Richard T. Carlin*[,‡]

Frank J. Seiler Research Laboratory, U.S. Air Force, Academy, Colorado 80840

Received: October 31, 1995; In Final Form: January 26, 1996[⊗]

To assess the effect of solvent on the properties of C_{60} anions, solutions of C_{60}^- and C_{60}^{3-} were generated electrochemically in 4:1 toluene:acetonitrile or DMSO containing 0.1 M tetrabutylammonium hexafluorophosphate. The anions were characterized by NIR spectroscopy and square-wave voltammetry. In both solvents continuous wave (CW) electron paramagnetic resonance (EPR) spectra at 8 K are axial for C_{60}^- and rhombic for C_{60}^{3-}, consistent with increasing distortion of the anion with increasing addition of electrons to the LUMO of C_{60}. The line shapes in the wings of the spectra, decreasing anisotropy of the spectra with increasing temperature, faster phase memory relaxation rates in the wings of the spectra, and distribution of values of the spin−lattice relaxation rate ($1/T_1$) provide evidence for a distribution of Jahn−Teller distorted forms and increasing rates of interconversion between these forms with increasing temperature. These properties are similar in the two solvents, despite substantial differences in solvent polarity. Extrapolation of the temperature dependence of $1/T_1$ measured below 30 K suggests that the line widths above 70 K are relaxation determined. Above about 70 K the line widths of the CW spectra broaden as increasing mobility of the solute/solvent increases the rate of spin−lattice relaxation.

Introduction

Calculations have shown that the LUMO of C_{60} is 3-fold degenerate.[1−4] The key to an understanding of the properties of anions derived from C_{60} is elucidation of the splitting of the t_{1u} LUMO by Jahn−Teller distortion for successive levels of reduction. This includes the need to understand the impact of solvation and/or counterion on the electronic energy levels. Kondo et al. reported differences between the near-IR (NIR) electronic spectra of C_{60}^- in nonpolar methylcyclohexane and in 2-methyltetrahydrofuran (MeTHF) at 77 K.[5] Stinchcombe et al. reported an axial EPR spectrum at 4 K of Na(crown)C_{60} in MeTHF and an isotropic EPR spectrum for the cobaltocene cation salt of C_{60}^- in THF.[6] The temperature dependence of the line widths in the EPR spectra of C_{60}^- above about 70 K has been observed to depend on solvent[7−9] and on cation in isolated solids.[10] Ion pairing has been suggested as a source of these environment effects. The extent of ion pairing may be solvent dependent.

In a previous paper we reported continuous wave (CW) EPR line shapes and preliminary electron spin relaxation data for C_{60}^- and C_{60}^{3-} generated electrochemically in 4:1 toluene:acetonitrile.[11] To examine the impact of solvent on the properties of C_{60} anions, we now report CW and time-domain EPR data for C_{60}^- and C_{60}^{3-} generated electrochemically in dimethyl sulfoxide (DMSO) and additional time-domain data for the toluene:acetonitrile solutions. One indication that DMSO and 4:1 toluene:acetonitrile provide substantially different solvation environments for C_{60} is the difference in solubilities in the two solvents. A 0.3 mM solution of C_{60} can be prepared readily in 4:1 toluene:acetonitrile, but C_{60} is essentially insoluble in DMSO. These observations are consistent with the report by Ruoff et al. that C_{60} is essentially insoluble in polar solvents although the solubility in toluene is about 4 mM at room temperature.[12] By examining CW line shapes and electron spin relaxation rates for both C_{60}^- and C_{60}^{3-} in two significantly different solvents from <10 K to as high a temperature as permitted by the lossy samples, we seek a more comprehensive understanding of the impact of solvent on the anions than has been possible previously.

Experimental Section

Electrochemical preparation of the C_{60} anions and characterization by electrochemistry and vis−NIR were performed at the Seiler Research Laboratory. EPR spectroscopy was performed at the University of Denver.

Electrochemistry and Vis−NIR Spectroscopy. C_{60} (99.5%) was obtained from Strem Chemicals and used without further purification. Tetrabutylammonium hexafluorophosphate ($TBAPF_6$) (Electronic Grade, Fluka) was dried at 110 °C under a vacuum of $<10^{-3}$ Torr for 72 h. Dimethyl sulfoxide (DMSO) (<0.1% H_2O, Aldrich), toluene (<0.005% H_2O, Aldrich), and acetonitrile (<0.005% H_2O, Aldrich) were kept over 4 Å molecular sieves (dried for 72 h at 400 °C and $<10^{-3}$ Torr) for several days prior to use. Solvents were filtered with a 0.2-μm PTFE filter (Whatman) to remove molecular sieve particulate prior to use.

Electrochemistry, vis−NIR spectroscopy, and EPR sample preparation were performed in a Vacuum Atmospheres drybox with O_2 and H_2O levels less than 1 ppm. Vis−NIR spectra were obtained *in situ* using a reflective fiber-optic dip probe as previously described.[11] The total optical path length for the probe is 0.382 cm. Square-wave voltammetry (SWV) and bulk electrolysis were performed as previously described.[11,13,14]

[†] Present address: Chemistry Department, U.S. Naval Academy, 572 Holloway Rd., Annapolis, MD 21402-5026.

[‡] Present address: Covalent Associates, Inc., 10 State St., Woburn, MA 01801.

[⊗] Abstract published in *Advance ACS Abstracts,* April 1, 1996.

0022-3654/96/20100-6910$12.00/0

Aliquots of the electrolysis solution were passed through a 0.45 μm PTFE filter to remove undissolved C_{60}, transferred to EPR tubes, attached to a manifold, removed from the glovebox, frozen in liquid nitrogen, and sealed with a torch. Except during EPR spectroscopy, the C_{60} anion samples were maintained at liquid nitrogen temperatures to maximize stability of the anions.

Suspensions of solid C_{60} in DMSO were prepared as previously described.[14] In the squarewave voltammograms of C_{60} in DMSO on a freshly polished GC electrode (Figure 1A in ref 14) a wave is observed at -1.03 V, which has twice the height of the following reduction steps and is at the potential expected for the $1-/2-$ couple.[14] This process is assigned to the direct two-electron conversion of C_{60} adsorbed on the electrode surface to C_{60}^{2-}. Electrolysis was performed at a voltage negative of the $1-/2-$ couple, and the NIR spectrum was monitored as a function of time. As the electrolysis proceeded, the peak at 1075 nm, characteristic of C_{60}^-, grew in intensity. The -1 anion is produced in solution via the homogeneous comproportionation reaction $C_{60} + C_{60}^{2-} \leftrightarrow 2\ C_{60}^-$. In the presence of C_{60} this equilibrium lies strongly to the right. Electrolysis was continued until the absorbance at 1075 nm was 1.2. Using an average literature value[11,15] of $\epsilon = 1.55 \times 10^4\ M^{-1}\ cm^{-1}$ and the 0.382 cm path length of the fiber-optic probe, this absorbance corresponds to 0.20 mM C_{60}^-. This is a 67% conversion of the total solid C_{60} added to the DMSO. An aliquot was withdrawn and filtered. Part of the filtered solution was transferred to EPR tubes, and part was diluted with toluene to produce a sample of C_{60}^- in 4:1 toluene:DMSO. Integration of the broad signal observed in the CW EPR spectra in DMSO at 105 K (see following section) gave the concentration of C_{60}^- as 0.18 mM, which is in good agreement with the concentration calculated from the NIR spectra. The low conversion of C_{60} to C_{60}^- is attributed to poor solubility in DMSO because further electrolysis of the same solution led to 87% conversion to C_{60}^{2-}.[14] The double integral of the CW EPR spectrum of the toluene:DMSO sample at 105 K was one-fifth of that observed for the DMSO solution before dilution, which demonstrated that the area of the broad signal changed linearly with dilution.

Bulk electrolysis to produce C_{60}^{3-} was performed at a voltage negative of the $2-/3-$ couple, on a solution that had been electrolyzed to produce C_{60}^{2-}. The NIR band at 950 nm, characteristic of C_{60}^{2-}, decreased as the intensity between 720 and 880 nm increased. The spectral changes are similar to those observed in 4:1 toluene:acetonitrile for conversion of C_{60}^{2-} to C_{60}^{3-}. [11] Electrolysis was continued until the absorbance at 788 nm showed no further change. Using the literature value[16] of $\epsilon = 1.4 \times 10^4$ at 788 nm, the observed absorbance (1.2) corresponds to a C_{60}^{3-} concentration of 0.22 mM, which is 73% conversion from the total solid C_{60} added to the DMSO. An aliquot was withdrawn and filtered. Part of the filtered solution was transferred to EPR tubes, and part was diluted with toluene. However, addition of toluene caused the color of the sample to change rapidly, indicating destruction of C_{60}^{3-}. Integration of the broad CW EPR spectra at 105 K in DMSO (see following section) gave the concentration of C_{60}^{3-} as 0.17 mM, which is in reasonable agreement with the NIR data. EPR spectra of the 4:1 toluene:DMSO sample at 105 K showed only a sharp signal with an integrated intensity that corresponded to a few percent of the total C_{60} in the sample. The C_{60}^{3-} appears to have been destroyed by reaction with trace impurities in the toluene.

The DMSO solutions containing C_{60}^- and C_{60}^{3-} were characterized by SWV. The voltammograms exhibited the expected oxidation and reduction waves.[11,14] To test the reversibility of the bulk electrolysis, the 0.22 mM solution of C_{60}^{3-} was oxidized to C_{60}^{2-}. The absorbance at 950 nm corresponded to 0.20 mM C_{60}^{2-}. Subsequent oxidation to C_{60}^- produced an absorbance at 1075 nm that corresponded to 0.18 mM C_{60}^-. These recoveries of higher oxidation states are less complete than when C_{60} was reduced to C_{60}^{2-} and then reoxidized.[14] This observation is consistent with earlier observations that C_{60}^{3-} is less stable than C_{60}^{2-},[8,11] but indicates that on the time scale of the bulk electrolysis the reduction process was largely reversible.

EPR Spectroscopy. Continuous wave (CW) spectra were recorded on a Bruker ESP380E or on a Varian E9. Two-pulse electron spin echo (ESE) and saturation recovery (SR) experiments were performed on the locally constructed spectrometers that have been described in the literature[17,18] or on the Bruker ESP380E. Data were obtained at frequencies between 9.1 and 9.7 GHz. On the locally constructed spectrometers temperatures below 77 K were obtained with an Oxford ESR900 flow cryostat and calibrated by substitution of a thermocouple in a sample tube in place of the EPR sample. On the ESP380E temperatures below 77 K were obtained with an Oxford ESR935 cryostat and calibrated with a Lakeshore 820 readout and a TG-120PL GaAlAs diode.[14] CW spectra at temperatures above 77 K were obtained on a Varian E9 with a liquid nitrogen flow system, and the temperature was monitored continuously with a thermocouple positioned above the sample. The g values were calculated from the microwave frequency measured with a microwave counter and the resonant magnetic field. The magnetic field readouts of the spectrometer field controllers were calibrated with DPPH ($g = 2.0036$) at room temperature. The uncertainty in g values is about ± 0.001 for the relatively narrow lines observed at low temperature. Relative g values within a spectrum are more accurate than the absolute values.

In the discussion of EPR data in this paper "integration" or "integral" implies double integration of the first-derivative CW spectrum to obtain the area under the corresponding absorption curve. Concentrations were determined by comparison of double integrals of CW spectra for C_{60} samples with double integrals of spectra of known concentrations of the stable nitroxyl radical 4-oxo-2,2,6,6-tetramethylpiperidin-1-oxyl (tempone, Aldrich Chemical) obtained under comparable conditions.

Values of the electron spin phase memory time, T_m, were calculated by fitting the spin−echo data to a single exponential of the form

$$y(\tau) = y(0)\ \exp(-(2\tau/T_m)^n) \qquad (1)$$

where τ is the interpulse spacing in the two-pulse experiment. In the fitting procedure the value of the exponent n was fixed at a specified value or adjusted in the least-squares fit. Saturation recovery curves were fit to a single exponential or to the sum of two exponentials using the algorithm of Provencher.[19]

Results

Electrochemical Generation and in Situ Characterization of C_{60}^- and C_{60}^{3-}. The generation and characterization by square-wave voltammetry and vis−NIR spectroscopy of C_{60}^- and C_{60}^{3-} in 4:1 toluene:acetonitrile were described previously.[11] The procedures developed to prepare C_{60}^{2-} in DMSO[14] were used to prepare C_{60}^- and C_{60}^{3-} in DMSO. Concentrations of C_{60}^- and C_{60}^{3-} determined from the intensity of characteristic bands in the NIR and double integration of the broad signals observed in the EPR spectra at 105 K were in reasonable agreement, as discussed in the preceding section.

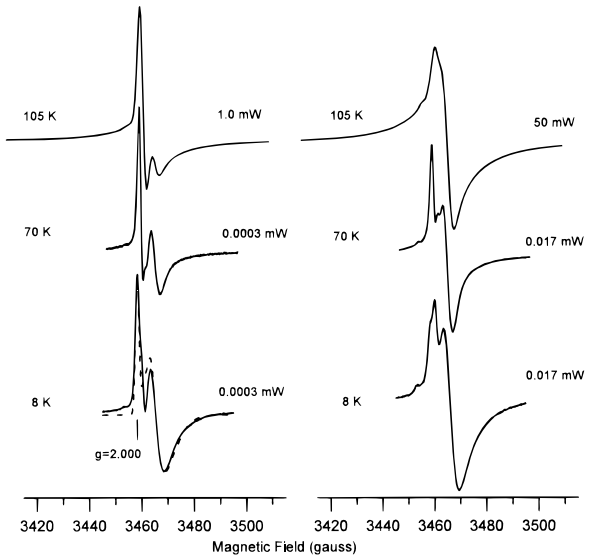

Figure 1. CW EPR spectra of C_{60}^- in DMSO solution containing 0.1 M $TBAPF_6$ as a function of temperature and microwave power at 9.17 GHz (105 K) and 9.69 GHz (8 and 70 K). Spectra taken at different frequencies were shifted horizontally to align corresponding *g* values. At each temperature, a lower power spectrum is shown on the left and a higher power spectrum is shown on the right. The microwave power is shown to the right of each spectrum. The modulation amplitude was 4.0 G at 105 K and 0.2 G at 70 and 8 K. The modulation frequency was 100 kHz at 105 K and 1.6 kHz at 70 and 8 K. The sharp peak in the 1.0 mW spectrum at 105 K was deliberately broadened by overmodulation to facilitate observation of the broad underlying signal. The simulation of the low-power spectrum at 8 K (- - -) is described in the text.

CW EPR Spectra of C_{60}^-. CW EPR spectra of C_{60}^- in DMSO as a function of temperature are shown in Figure 1. Comparable spectra of C_{60}^- in 4:1 toluene:acetonitrile are shown in Figure 9 of ref 11. At 8 K the spectrum recorded with 0.0003 mW of microwave power appears axial (Figure 1). As temperature is increased above about 40 K, most of the features of the spectrum broaden, analogous to what has been observed in other samples of C_{60}^-.[6,7,11,15,20] The low-power spectra at 70 and 105 K show a sharp peak superimposed on an increasingly broad signal. At these temperatures the two contributions are more readily distinguished than at 8 K, and at 105 K integrations show that the sharp signal accounts for less than 5% of the total signal intensity. The sharp signal saturates much more readily than the broad component, so its contribution to the CW spectra is smaller at higher microwave powers than at low microwave power (Figure 1). At 8 K when the microwave power is increased from 0.0003 to 0.017 mW, the relative intensity of the low-field edge of the signal decreases, so this is assigned as the region in which the slower relaxing signal that stays sharp at higher temperatures contributes. However, the intensity of that signal is too small to account for all of the intensity at the low-field peak of the spectrum. The low-field *g* value for C_{60}^- is approximately superimposed on the sharp signal.

At 4 K, using the lowest microwave power available on the spectrometers (200 nW), the integrated intensity of the CW spectrum did not increase linearly with square root of microwave power so it was not possible to obtain unsaturated spectra to quantitative signal intensity. Unsaturated spectra were obtained above about 10 K, and the integrated intensity of the broad signal in 4:1 toluene:acetonitrile or in DMSO decreased linearly with $1/T$.

As has been discussed previously for spectra of C_{60}^- obtained in other solvents,[6,11] computer simulations based on standard models for rigid-lattice spectra do not give good agreement with the experimental data. The simulation of the spectrum of C_{60}^- at 8 K (Figure 1) was obtained with an empirical model. The line shape varied from Gaussian with a width of 1.1 G at the low-field extrema to Lorentzian with a width of 14 G at the high-field edge. A Gaussian distribution of *g* values was approximated as a distribution in resonant fields. The width of the distribution varied from 1 G at the low-field edge to 8.5 G at the high-field edge. The simulated spectrum is sensitive to the functional form that is used to describe the field/orientation dependence of line width, line shape, and width of the Gaussian distribution, and we found that to match the observed spectra all three must vary. A physical model for these variations will be needed before the simulation can be optimized, however, the agreement between simulation and experiment that is shown in Figure 1 is substantially better than what has been obtained previously without invoking distributions.[6,11] With increasing temperature the *g* anisotropy decreases, and the width of the Gaussian distribution of *g* values that is required to match the high-field wing of the spectrum decreases.

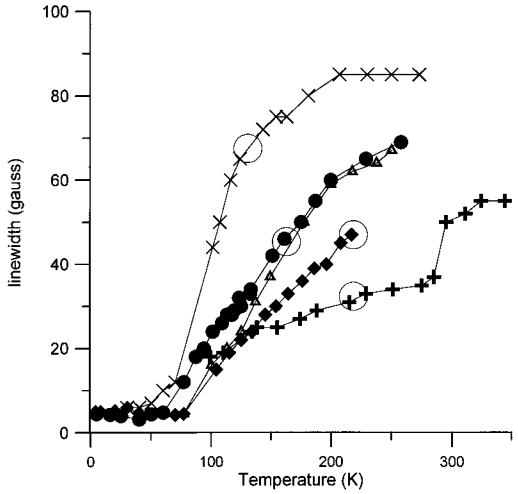

Figure 2. Temperature dependence of CW line widths for C_{60}^- at 9.1−9.2 GHz: (+) chemically prepared K^+ salt in DMSO; (×) chemically prepared Ca^{2+} salt in MeTHF; samples prepared electrochemically in (◆) DMSO; (△) 4:1 toluene:DMSO; and (●), 4:1 toluene:acetonitrile. The lines in the plot connect the data points. The line widths for the chemically prepared samples are reproduced from ref 7. The electrochemically prepared samples contained 0.1 M $TBAPF_6$. The circled regions on each line encompass the temperature interval in which the CW spectra of tempo in the same solvent showed a transition from "immobilized" to rapid tumbling (see text for details).

Above about 70 K the line width of the C_{60}^- signal in DMSO increased with increasing temperature. The broader lines cause increased uncertainty in the integrations, but the integrated intensity was approximately proportional to $1/T$. The line shapes at temperatures above about 70 K are broader in the wings of the spectrum than can be fit with a single Lorentzian line that matches the peak-to-peak width of the spectrum.[7] Computer simulations were performed with a Gaussian distribution of Lorentzian line widths with a 5 to 15 G distribution width. The central value of the distribution is plotted in Figure 2 as a function of temperature for samples in DMSO or 4:1 toluene:DMSO. Line width data as a function of temperature from refs 7 and 11 are included in Figure 2 for comparison. Samples studied in refs 7 and 11, as well as in this paper, were contained in 4 mm o.d. quartz tubes. For long columns of sample in these tubes the lossiness of DMSO above the melting point or of 4:1 toluene:acetonitrile above the softening point of the glass was too great to tune the EPR spectrometer. In ref 7 short columns

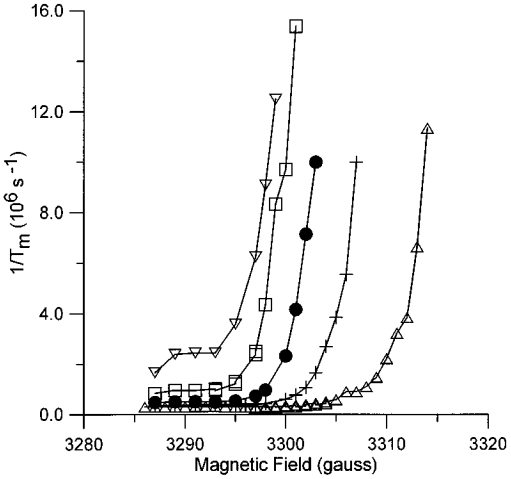

Figure 3. Magnetic field dependence of $1/T_m$ for C_{60}^- in 4:1 toluene:acetonitrile containing 0.1 M $TBAPF_6$ as a function of temperature at 9.21 GHz: (△) 9, (+) 18, (●) 27, (□) 36, and (▽) 45 K. Spin−echo data were obtained with a 90°−180° pulse sequence using 30 and 60 ns pulses. Data were fitted to a single exponential with an exponent of 1.0.

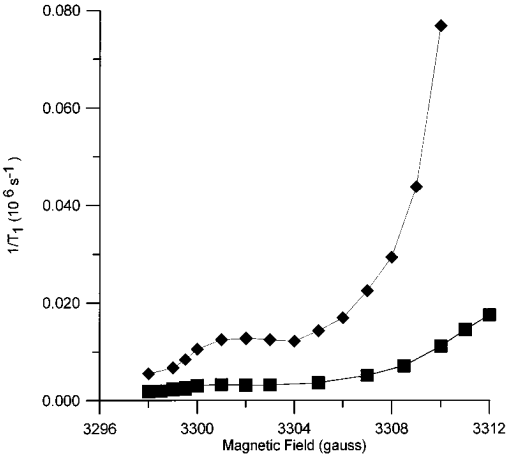

Figure 4. Magnetic field dependence of $1/T_1$ for C_{60}^- in 4:1 toluene:acetonitrile containing 0.1 M $TBAPF_6$ at 9.21 GHz: (◆) 17 and (■) 8 K. Saturation recovery data were fitted to a single exponential with an exponent of 1.0.

of solution (about 5 mm high in the 4 mm o.d. tubes) permitted EPR measurements in DMSO solution up to 350 K.

ESE Measurements on C_{60}^-. Two-pulse ESE data obtained for C_{60}^- in 4:1 toluene:acetonitrile were fit to a single-exponential decay. The resulting time constant is denoted as T_m to encompass all processes that contribute to dephasing of the spin echo. Values of $1/T_m$ as a function of position in the spectrum at a series of temperatures are shown in Figure 3. The phase memory relaxation rate is dramatically faster in the high-field wing of the spectrum. The shift in the high-field extrema toward lower field (higher g value) with increasing temperature that was noted in the CW spectrum is reflected in the ESE data as a shift toward lower field of the more rapidly relaxing components of the spectrum. Field-swept echo-detected spectra also demonstrated the decrease in g anisotropy with increasing temperature. The slower relaxing sharp component that was observed in the CW spectra made a negligibly small contribution to the ESE decays at most temperatures. T_1 for the sharp signal is so much longer than T_1 for the broad signal that the magnetization from the sharp signal does not recover effectively at the pulse repetition rates used to record the ESE data. However, the sharp signal was the source of the slower relaxing signal observed at 3286 G at 45 K. Above about 45 K $1/T_m$ for the broad signal became so fast that even for small values of interpulse spacing, field-swept echo-detected spectra showed only the residual contribution from the sharp signal. In addition to the change in time constant, the shapes of the echo decays were dependent upon position in the spectrum. Near the low-field end of the spectrum the best fits to the data were obtained with an exponent (n in eq 1) about 1.2. Toward the high-field wing of the spectrum the best-fit exponent decreased to about 0.5. The smaller exponent is characteristic of a system undergoing a dynamic process. The values of T_m in Figure 3 were obtained with the exponent fixed at 1.0. The variation in decay time constant with position in the spectrum was even larger than shown in Figure 3 when the exponent was allowed to vary.

The CW spectra for C_{60}^- in 4:1 toluene:acetonitrile (Figure 9 of ref 11) and in DMSO (Figure 1) are very similar at temperatures up to about 77 K. However, ESE measurements are more sensitive to local spin concentration than are CW spectra. In 4:1 toluene:acetonitrile the value of T_m for a 0.2 mM sample of C_{60}^- at 8 K was independent of pulse turning angle, which indicates that instantaneous diffusion makes a negligible contribution to the phase memory decay.[21,22] Negligible contribution from instantaneous diffusion is consistent with the bulk concentration of C_{60}^- (about 0.2 mM) in the sample. However, in DMSO for approximately the same concentration of C_{60}^-, the values of T_m were dependent upon turning angle, which showed that the local spin concentration was higher than the bulk concentration. This observation suggests that crystallization of the solvent caused nonuniformity in solute concentration. The observation of an anisotropic low-temperature spectrum in DMSO (Figure 1) indicates that the average local spin concentration was not so high as to cause exchange averaging of the g anisotropy. In DMSO the values of T_m for C_{60}^- were only weakly dependent on position in the spectrum and were approximately equal to the weighted averages of the orientation-dependent values obtained in 4:1 toluene:acetonitrile (Figure 3). The smaller orientation dependence of $1/T_m$ in DMSO also is attributed to extensive communication between the spins due to the higher local concentration in DMSO than in 4:1 toluene:acetonitrile for the same bulk concentration.

SR Measurements on C_{60}^-. In 4:1 toluene:acetonitrile or DMSO the values of $1/T_1$ determined by SR for C_{60}^- are strongly dependent upon position in the spectrum (Figure 4). The fastest relaxation rates are observed at the high-field end of the spectrum. To show the trends in the data, the values plotted in Figure 4 were obtained by fitting the experimental data to a single exponential. However, the saturation recovery curves are not single exponentials. Analysis of the data by fitting to a sum of exponentials indicates that the recovery curves are due to a distribution of exponentials.[11]

Figure 5 summarizes the relaxation rate data obtained in the center of the spectra as a function of temperature for C_{60}^- in MeTHF,[7] 4:1 toluene:acetonitrile,[11] and DMSO. The values of $1/T_1$ are similar in the three solvents, are strongly temperature dependent, and become too short to measure using our spectrometers above about 25 K. Values of $1/T_m$ in the center of the spectrum are weakly temperature dependent below about 25 K. The trends in the values of $1/T_1$ and $1/T_m$ imply that above about 30 K $T_1 = T_m$, and this value is assumed to be equal to T_2. Above about 70 K the line widths become temperature dependent. The temperature-dependent contributions to the line widths can be used to estimate $1/T_2$, and these values are included in Figure 5. The solid line in Figure 5 is a linear least-square fit to the values of $1/T_1$ obtained by SR at

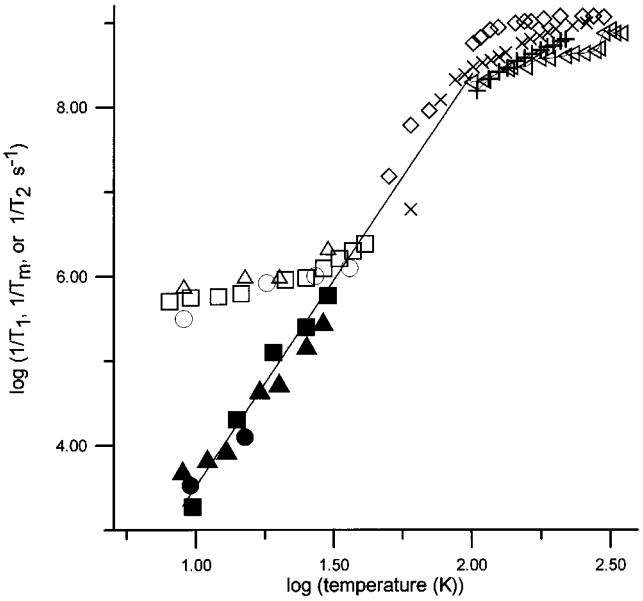

Figure 5. Temperature dependence of electron spin relaxation rates at X-band (9.1−9.2 GHz) for C_{60}^-. Average T_1 measured by SR in (■) MeTHF, (●) 4:1 toluene:acetonitrile, or (▲) DMSO. T_m measured by ESE in (□) MeTHF, (○) 4:1 toluene:acetonitrile, or (△) DMSO. T_2 calculated from temperature-dependent contribution to line widths in (◇) MeTHF, (×) 4:1 toluene:acetonitrile, or (+, rotated △) DMSO. The solid line is a fit to the combined SR and line width data and has a slope of 4.88.

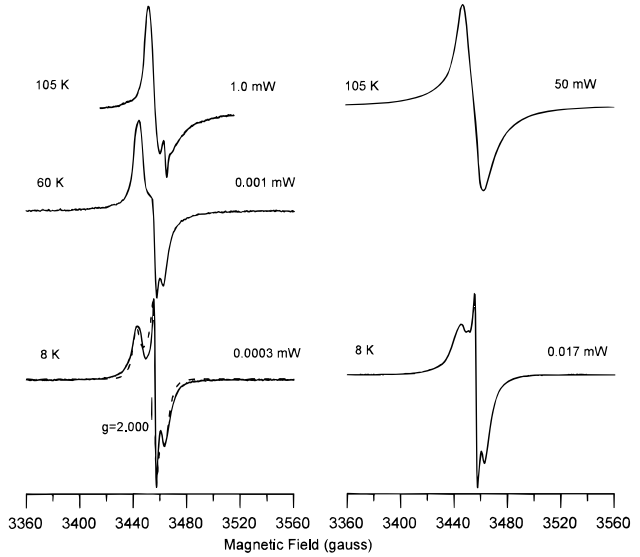

Figure 6. CW EPR spectra of C_{60}^{3-} in DMSO containing 0.1 M $TBAPF_6$ as a function of temperature and microwave power at 9.17 GHz (105 K) and 9.69 GHz (8 and 60 K). Spectra taken at different frequencies were shifted horizontally to align corresponding g values. Spectra at lower power are shown on the left, and spectra at higher power are shown on the right. The microwave power is shown to the right of each spectrum. The modulation amplitude was 4.0 G at 105 K, 0.5 G at 70 K, and 0.1 G at 8 K. The modulation frequency was 100 kHz at 105 K and 1.6 kHz at 60 and 8 K. The simulated spectrum (− − −) was calculated with g = 2.008, 2.000, and 1.995 and anisotropic Lorentzian line widths of 4.0, 1.5, and 4.5 G, respectively.

low temperature and the values of $1/T_2$ calculated from the high temperature line widths.

CW EPR of C_{60}^{3-}. CW EPR spectra of C_{60}^{3-} in DMSO as a function of temperature are shown in Figure 6. Comparable spectra of C_{60}^{3-} in 4:1 toluene:acetonitrile are shown in Figure 13 of ref 11. In the spectrum of C_{60}^{3-} in DMSO at 8 K the g values are approximately 2.008, 2.000, and 1.995. The relative intensity of the sharp feature in the center of the spectrum varies with sample preparation, which shows that it is due, at least in part, to another species. This observation raises the question whether the spectrum of C_{60}^{3-} is axial or rhombic; i.e., is there a g value for C_{60}^{3-} at about 2.000, or are all of the features near g = 2.000 due to another species? Several pieces of evidence indicate that the spectrum of C_{60}^{3-} is rhombic and includes a g value near 2.000. (1) It is easier to distinguish the sharp signal from the rest of the signal at higher temperatures where the signal from the C_{60}^{3-} is broader. The relative intensity of the sharp signal at higher temperatures is a few percent of the total EPR intensity, which is too small to account for all of the intensity in the center of the low-temperature spectrum. Thus, only part of the intensity at g = 2.000 is due to the signal that remains sharp with increasing temperature. (2) The sharp signal that is observed at higher temperatures exhibits much slower electron spin relaxation than the rest of the spectrum as can be seen from its prominent contribution to the 1.0 mW spectrum and nearly negligible contribution to the 50 mW spectrum at 105 K. Increasing the microwave power from 0.0003 to 0.017 mW at 8 K had a much smaller impact on the relative intensity of the signal at g = 2.000 than at 105 K, which indicates that the relaxation behavior of most of the signal that contributes at g = 2.000 is similar to that of the rest of the signal. Direct measurements of $1/T_1$ (described below) confirm that the spin−lattice relaxation rate for most of the signal in the center of the spectrum is similar to that for the rest of the spectrum. (3) Computer simulations of the line shape at 8 K could not match the relative intensities of the turning points at 2.008 and 1.996 with an axial spectrum. The simulation shown in Figure 6 was obtained with rhombic g values. Simulations of the spectra of C_{60}^{3-} in 4:1 toluene:acetonitrile also gave better agreement with experiment for rhombic g values than for axial g values.[11] The combined data argue that in both solvents the spectra of C_{60}^{3-} are rhombic. The signal that remains sharp at high temperature makes a relatively small contribution to the low-temperature spectra. Even with the Lorentzian line widths used in the simulation shown in Figure 6, the intensity in the wings of the experimental spectrum is greater than that in the simulation. A distribution of g values due to a distribution of Jahn−Teller distortions, analogous to what was used to simulate the spectra of C_{60}^-, may also be need to optimize the fit to the spectrum of C_{60}^{3-}.

As temperature was increased, the extrema in the CW spectra moved toward the center of the spectrum (Figure 6). The difference between the highest and lowest g values decreased from about 0.012 at 8 K to about 0.010 at 70 K. A similar temperature dependence of g values was observed in 4:1 toluene:acetonitrile.[11] As the temperature was increased above about 70 K, the line widths of the spectra broadened. Simulations of the spectra above 70 K were obtained with an isotropic g value and a Gaussian distribution of Lorentzian line widths. The central line width of the distribution is plotted in Figure 7 for samples in 4:1 toluene:acetonitrile and in DMSO. Between 80 and 140 K the line widths in 4:1 toluene:acetonitrile were consistently broader than the line widths in DMSO.

Electron Spin Echo Measurements on C_{60}^{3-}. Two-pulse ESE data were obtained for C_{60}^{3-} in 4:1 toluene:acetonitrile (Figure 8). The values of $1/T_m$ were strongly dependent upon position in the spectrum with faster relaxation rates observed in both the high-field and low-field wings of the spectrum and slower rates observed in the center. In addition to the change in time constant, the shapes of the echo decays were dependent upon position in the spectrum. Near the center of the spectrum the best fits to the data were obtained with an exponent (n in

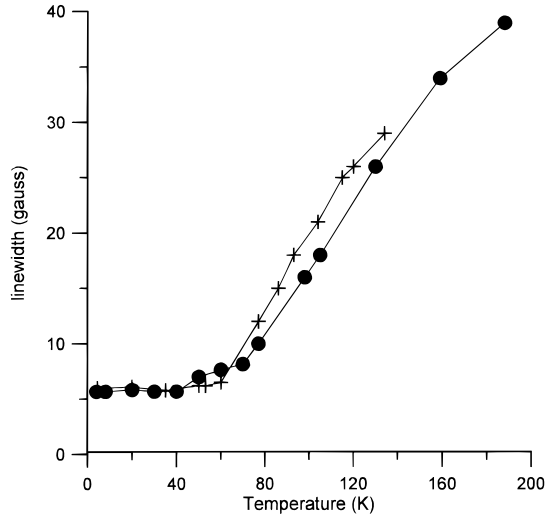

Figure 7. Temperature dependence of CW line widths at 9.1−9.2 GHz for electrochemically prepared C_{60}^{3-} in (●), DMSO or (+) 4:1 toluene: acetonitrile. The lines in the plot connect the data points. Both solvents contained 0.1 M $TBAPF_6$.

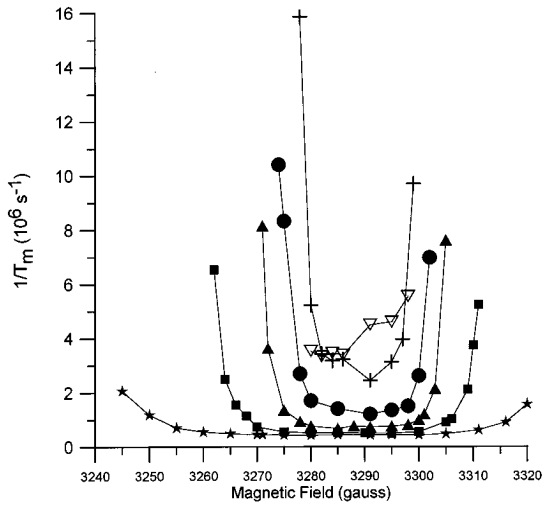

Figure 8. Magnetic field dependence of $1/T_m$ for C_{60}^{3-} in 4:1 toluene: acetonitrile as a function of temperature at 9.21 GHz: (★) 7, (■) 10 (▲) 18 (●) 27, (+) 36, and (▽) 45 K. Spin−echo data were obtained with a 90°−180° pulse sequence using 30 and 60 ns pulses. Data were fitted to a single exponential with an exponent of 1.0.

eq 1) about 1.2. Toward the low-and high-field wings of the spectrum the best-fit exponent decreased to about 0.5. The smaller exponent is characteristic of systems undergoing a dynamic process. The values of T_m in Figure 8 were obtained with the exponent fixed at 1.0. The variation in decay time constant with position in the spectrum was even larger than shown in Figure 8 when the exponent was allowed to vary. At lower temperatures the sharp signal that is observed in the CW spectrum makes a negligible contribution to the echo decays. T_1 for the sharp signal is so much longer than T_1 for the broad signal that the magnetization for the sharp signal does not recover effectively at the pulse repetition rates used to record the ESE data. However, at 45 K the phase memory relaxation rate for the broad signal is so fast that the sharp signal is a major contribution to a two-pulse field-swept echo-detected spectrum. The contribution from the sharp signal is the source of the longer relaxation rate measured at about 3280 G at 45 K (Figure 8).

The values of $1/T_m$ for C_{60}^{3-} in DMSO were dependent upon pulse turning angle. This dependence indicates significant instantaneous diffusion that is characteristic of a local concentration that is higher than the 0.20 mM bulk concentration. The value of $1/T_m$ obtained with small turning angle in the center of the spectrum in DMSO was faster than in 4:1 toluene: acetonitrile. For example, at 10 K $1/T_m$ in DMSO was 1.2×10^6 s^{-1} and in 4:1 toluene:acetonitrile the value was 0.5×10^6 s^{-1}. The dependence of $1/T_m$ on position in the spectrum was smaller in DMSO than in 4:1 toluene:acetonitrile. For example, at 10 K the ratio of $1/T_m$ at magnetic fields 20 G above or below the center of the spectrum to that at the center was about 6 in toluene:acetonitrile and about 1.5 in DMSO. These differences between samples in toluene:acetonitrile and DMSO are attributed to locally high concentrations of solute that arise from crystallization of the DMSO.

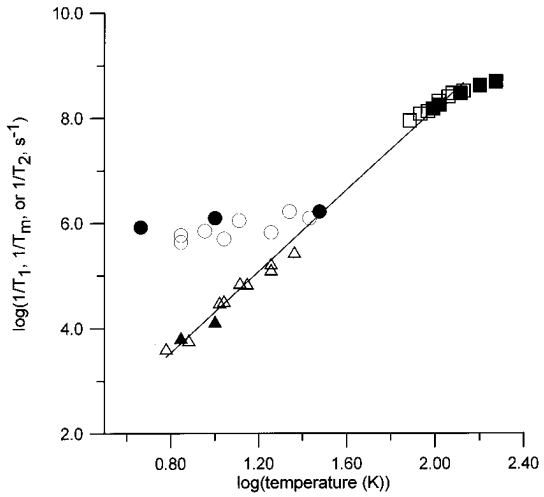

Figure 9. Temperature dependence of electron spin relaxation rates at X-band (9.1−9.2 GHz) for C_{60}^{3-} prepared electrochemically in 4:1 toluene:acetonitrile: (△) average T_1 measured by SR; (○) T_m measured by ESE; (□) T_2 calculated from temperature-dependent contribution to line widths; and in DMSO: (▲), average T_1 measured by SR, (●) T_m measured by ESE; and (■), T_2 calculated from temperature-dependent contribution to line widths. The solid line is a fit to the combined SR and line width data and has a slope of 3.87.

Saturation Recovery Measurements on C_{60}^{3-}. In 4:1 toluene:acetonitrile or DMSO the SR curves for C_{60}^{3-} were not single-exponential decays. Analogous to the observations for C_{60}^- the data indicate the presence of a wide distribution of values of $1/T_1$. As discussed previously, this distribution is too large to be due to the temperature variation over the length of the sample.[11] Instead, it is assigned to a distribution of anions with different distortions from I_h symmetry. In contrast to the observations for C_{60}^-, the values of T_1 for C_{60}^{3-} in 4:1 toluene: acetonitrile or DMSO showed little dependence upon position in the spectrum.

Figure 9 summarizes the relaxation rate data as a function of temperature obtained in the center of the spectra for C_{60}^{3-} in 4:1 toluene:acetonitrile and DMSO. The pattern is similar to that observed for C_{60}^{1-} (Figure 5). The values of $1/T_1$ obtained in both solvents are strongly temperature dependent. Values of $1/T_m$ in the center of the spectrum are weakly temperature dependent below about 25 K. Above about 30 K $T_1 \sim T_m$, and this value is assumed to be equal to T_2. Above about 70 K the line widths become temperature dependent. Above 70 K $1/T_2$ was calculated from the temperature-dependent contributions to the line widths. The solid line in Figure 9 is a linear least-squares fit to the values of $1/T_1$ obtained by SR at low temperature and the values of $1/T_2$ calculated from the high temperature line widths.

Temperature Dependence of Nitroxyl Line Shapes. The CW EPR line shape of the stable nitroxyl radical tempo (2,2,6,6-tetramethylpiperidin-1-oxyl) was used as a probe of the tem-

perature-dependent mobility of a small low-polarity molecule in the solvents used to study the C_{60} anions. When the tumbling correlation time of a nitroxyl radical is longer than about 10^{-8} s, an "immobilized" anisotropic EPR spectrum with a characteristic nitrogen hyperfine splitting (a_{zz}) of about 35 G is observed. When the nitroxyl has a tumbling correlation time shorter than about 10^{-11} s, an isotropic spectrum with a nitrogen hyperfine splitting of about 16 G is observed.[23] Spectra of 0.1−0.3 mM tempo solutions in MeTHF, in 4:1 toluene:acetonitrile containing 0.1 M $TBAPF_6$, in DMSO, and in DMSO containing 0.1 M $TBAPF_6$ were recorded as a function of temperature. In each of the solvents the nitroxyl line shape changed from the "immobilized" to the rapidly tumbling regime within about a 20 K interval. Those temperature intervals are shown as circles in Figure 2. Rapid freezing of a 0.1 mM tempo solution in DMSO resulted in a typical immobilized spectrum. However, as the solution was warmed to about 200 K, the spectrum changed to a broad signal without resolved nitrogen hyperfine coupling, which is characteristic of incomplete exchange narrowing in a magnetically concentrated sample. This line shape change was not reversible on cooling the sample. Further warming led to a rapidly tumbling spectrum, below the "melting point" of the DMSO. At lower tempo concentration (0.03 mM) the line shape did not change when the sample was warmed through 200 K. We propose that a phase change occurs at approximately 200 K that results in exclusion of solute from the new lattice. At higher initial solute concentrations, the local spin concentration can become high enough to cause partial exchange averaging of the nitrogen hyperfine interaction. For 0.1 mM tempo in DMSO containing 0.1 M $TBAPF_6$ this change in the nitroxyl line shape at 200 K did not occur, which suggests that the high ion concentration changes the phase behavior of the DMSO. Although we are not aware of reports concerning the effect of ionic solutes on DMSO, the addition of $LiClO_4$ to water is a well-documented way to prepare low-temperature glassy aqueous samples. Although the cooled solutions of DMSO containing $TBAPF_6$ were not optically clear, the solutions do not tend to crystallize as extensively as in the absence of electrolyte.

Based on visual inspection of the mobility of an object in the solvents during a slow warming process, the approximate temperatures at which there is substantial macroscopic mobility are as follows: MeTHF, 130 K; 4:1 toluene:acetonitrile containing 0.1 M $TBAPF_6$, 180 K; DMSO, 290 K. For toluene:acetonitrile and DMSO these temperatures were about 20 and 70 K higher, respectively, than the midpoint of the temperature range in which the tempo spectra showed the transition from "immobilized" to rapid tumbling. For this set of solvents it appears that as the melting/softening temperature increases, there is a larger discrepancy between the temperature at which there is local mobility of the nitroxyl and the melting/softening temperature.

Discussion

The integrated intensities of the broad signals observed for C_{60}^- and C_{60}^{3-} in DMSO and 4:1 toluene:acetonitrile were proportional to $1/T$ as expected for a ground state. The overlap between the broad and sharp signals makes it difficult to obtain valid integrals for the sharp signal. However, the line shape of the sharp signal in DMSO solution shows little temperature dependence between 110 and 220 K, so peak height is a valid monitor of the temperature dependence of signal intensity. In this temperature interval the intensity of the sharp signal was proportional to $1/T$, as expected for the signal from a ground state. This temperature dependence[14] is inconsistent with the proposal that the low-intensity sharp signal in the EPR spectra of C_{60}^- samples is due to a thermally-accessible excited state.[6] The line shape of the spectrum of C_{60}^- in 4:1 toluene:DMSO at 105 K was similar to that observed in DMSO at the same temperature, and the relative intensity of the sharp signal was unchanged by dilution. It has been proposed that the species that give the broad and sharp signals are in equilibrium.[6] If that is the case, the equilibrium is not strongly solvent or concentration dependent. The emphasis of this paper is on the broad signals that account for more than 95% of the total signal area.

Dynamic Jahn−Teller Distortion. If the I_h symmetry of C_{60} is retained upon reduction to C_{60}^-, and there is no Jahn−Teller distortion of C_{60}^-, the EPR spectrum of C_{60}^- would be isotropic. Jahn−Teller distortions of C_{60}^- via the h_g vibrational mode can result in structures having D_{5d}, D_{3d}, or D_{2h} symmetry.[24] It has been calculated that the energies of these distorted forms are nearly degenerate[24] and lower than that of the higher-symmetry I_h form.[24,25] NIR spectra of C_{60}^- at 77 K have been interpreted as indicating a preference for the D_{2h} form in polar MeTHF and either the D_{5d} or the D_{3d} geometry in nonpolar matrices. Each of the proposed distorted structures has axial symmetry, which predicts an axial EPR spectrum.

CW EPR spectra of C_{60}^- generated electrochemically in DMSO are shown in Figure 1. The spectrum at 8 K is axial and is similar to those reported previously at temperatures below 10 K for samples of C_{60}^- prepared electrochemically in 4:1 toluene:acetonitrile[11] or CH_2Cl_2[15] and for solutions of chemically prepared salts of C_{60}^-: $Cr(TTP)(C_{60})(THF)_3$ in THF,[20] Na(crown)C_{60} in MeTHF,[6] KC_{60} in MeTHF,[7] and $Ca(C_{60})_2$ in MeTHF.[7] The axial spectra support the assignment of the structure as Jahn−Teller distorted.[15,26] The substantial similarities between these spectra provide no evidence for a strong solvent dependence of the distortion. However, the spectrum of the cobaltocene cation salt of C_{60}^- in THF at 4 K appears to be isotropic.[6] Since THF does not form a glass when cooled, one possible explanation for the isotropic signal in this solvent is a high local concentration of solute. The possibility of higher symmetry for this salt cannot be ruled out without data in a solvent that forms a glass.

The average g values for C_{60}^- at 8 K are 1.995 in 4:1 toluene:acetonitrile[11] and 1.996 in DMSO, which are the same within our experimental uncertainty. The g values less than 2.002 observed for C_{60}^- are attributed to spin−orbit coupling that results from Jahn−Teller distortion of the t_{1u} LUMO of C_{60}.[15,26,27] As discussed in the preceding section, simulation of the low-temperature spectra is improved by using a distribution of g values that is larger in the equatorial plane than along the principal axis. This distribution in g values is attributed to a distribution in Jahn−Teller distortions. Species with the least distortion have g values further from 2.002 and the most distorted forms have g values closer to 2.002.[11]

The CW spectra of C_{60}^{3-} generated electrochemically in DMSO (Figure 6) are similar to those observed for C_{60}^{3-} in 4:1 toluene:acetonitrile.[11] The spectra at 8 K are rhombic, which indicates that the symmetry of C_{60}^{3-} is lower than that of C_{60}^-. However, the spectrum of a salt of C_{60}^{3-} dissolved in DMSO (figure 4 of supplementary material for ref 28) did not show anisotropy at 4 K. As noted in the discussion of the spectra of tempo in DMSO, we have observed that the tendency of solute to become magnetically concentrated in frozen DMSO depends upon solute concentration as well as the presence/absence of supporting electrolyte. A possible explanation for the absence of anisotropy in the EPR spectrum of C_{60}^{3-} in DMSO reported in ref 28 is exclusion of solute from the lattice during

crystallization. The locally high concentration could cause exchange averaging of the *g* anisotropy. The EPR spectrum of C_{60}^{3-} in DMSO broadens with increasing temperature[28] analogous to what is observed for C_{60}^{3-} in DMSO or toluene: acetonitrile containing supporting electrolyte. Relatively weak electron−electron spin exchange could average the *g* anisotropy without altering the electronic structure that contributes to the rapid electron spin relaxation at higher temperatures.

As temperature is increased to about 70 K, the *g* anisotropy in the spectra of both C_{60}^- and C_{60}^{3-} decreases. For C_{60}^- the high-field feature moves toward higher *g* value. For C_{60}^{3-} the low-field and high-field extrema move toward the middle *g* value. It has been proposed that the narrowing of the spectrum of C_{60}^- is due to dynamic averaging of different Jahn−Teller distorted forms.[6,11,15] The range of solvents in which this narrowing has been reported suggests that this is a general phenomenon for C_{60}^-. We suggest that this also is a plausible explanation for the narrowing of the C_{60}^{3-} spectrum with increasing temperature to about 70 K. This process can be viewed as a pseudorotation. For C_{60}^- the broader line width and wider distribution of *g* values are observed for the high-field component of the signal. This is the *g* value that is further from 2.002. It is most sensitive to the Jahn−Teller distortion and moves toward $g = 2.000$, the component with the narrower line width, as the distorted forms average. For C_{60}^{3-} both the low-field and high-field *g* values are sensitive to the extent of distortion, and the line widths at these *g* values are broader than at the central *g* value. As the various distorted forms average, the extreme *g* values move toward the center. The variations in line widths can be viewed as an example of what is commonly called "*g* strain".

The ESE measurements gave phase memory relaxation times in the wings of the spectra of the order of 0.1 μs, which corresponds to a spin-packet width of 0.66 G. This spin-packet width is an order of magnitude smaller than the line width required to approximately match the experimental spectra, so at low temperature the line widths are not relaxation time determined. At low temperatures the Lorentzian line shapes in the high-field wing of the C_{60}^- spectra and in both high-field and low-field wings of the C_{60}^{3-} spectra imply that the line shape is lifetime determined. The spin-echo data indicate that the relevant lifetime is not the spin relaxation. Rather, the lifetime may be the determined by the interconversion of nearly equivalent Jahn−Teller distorted forms.

The values of $1/T_m$ obtained for C_{60}^- by ESE (Figure 3) are substantially faster in the high-field wing than in the rest of the spectrum. A dynamic process that moves a spin packet off resonance on the time scale of the ESE measurement (microseconds) is a dephasing process that results in an increase in $1/T_m$. Thus, the observation of enhanced values of $1/T_m$ in the high-field wing of the spectrum is consistent with assignment of this portion of the spectrum to anions for which the resonant magnetic field is sensitive to interconversion between distorted forms. The values of $1/T_m$ for C_{60}^{3-} (Figure 8) are faster in both wings of the spectrum than in the center of the spectrum. Similar to the arguments for C_{60}^-, in the wings of the spectra of C_{60}^{3-} the resonance field is most sensitive to the effects of the dynamic interconversion process, which results in faster $1/T_m$. The proposal that there is a distribution of distortions for both C_{60}^- and C_{60}^{3-} also is supported by the wide distribution of values of T_1 observed at each position in the spectrum in MeTHF,[7,11] 4:1 toluene:acetonitrile,[7,11] or DMSO.

Orientation Dependence of T_1. For C_{60}^- the orientation dependence of $1/T_1$ and $1/T_m$ was similar (Figures 3 and 4). For C_{60}^{3-} $1/T_1$ was approximately independent of position in the spectrum, although $1/T_m$ was strongly position dependent (Figure 8). This contrast suggests that the orientation dependence of $1/T_1$ for C_{60}^-, and absence of orientation dependence of $1/T_1$ for C_{60}^{3-} is due to something other than the motional effects that cause the orientation dependence of $1/T_m$ for both anions. In axial $S = {}^1/_2$ spin systems as diverse as the E′ defect center in irradiated fused quartz,[29] nitroxyl radicals,[30] bis-(diethyldithiocarbamato)copper(II),[31] chromium(V) porphyrins,[32] and molybdenum(V) porphyrins,[33] it has been observed that $1/T_1$ is faster in the equatorial plane than along the unique axis. The orientation dependence is attributed to the larger number of vibrational modes in the equatorial plane and to the greater impact of spin−orbit coupling on *g* values in the equatorial plane.[30,32] Anisotropy of $1/T_1$ has not been observed in closely related systems that are rhombic.[34] This model is consistent with the observation of orientation dependence of $1/T_1$ for axial C_{60}^- and not for rhombic C_{60}^{3-}.

Temperature Dependence of Line Widths above 70 K. For both C_{60}^- and C_{60}^{3-} above about 70 K the line widths of the EPR spectra in DMSO and 4:1 toluene:acetonitrile increase with increasing temperature (Figures 2 and 7). Increasing line widths with increasing temperature above about 70 K also have been reported for electrochemically generated C_{60}^- studied in other frozen/glassy solutions,[8,35,36] for solutions of C_{60}^- salts,[6,7,37] for solid C_{60}^- salts,[10,26,38−43] for C_{60}^{3-} generated electrochemically in benzonitrile, CH_2Cl_2, and pyridine,[8] for a solid C_{60}^{3-} salt,[44] and for a salt of C_{60}^{3-} dissolved in DMSO.[28] Above the melting point of the solvents line widths are in the range 60−90 G and are less temperature dependent than in the frozen/glassy state.[7,9] In solid samples the line widths generally are still increasing at 300 K, and line widths between about 10 and 50 G have been reported.[40]

Several models have been proposed to explain the temperature-dependent line widths. It has been suggested that interaction of the matrix with C_{60}^- causes partial removal of the 3-fold degeneracy of the C_{60} LUMO.[9] When the solvent melts, this interaction is weakened, restoring higher symmetry and faster relaxation.[9] Another proposal is that the temperature dependence is due to increasing rates of thermal averaging over two electronic states.[8] The observation of thermally accessible electronic excited states for C_{60}^{2-} and C_{84}^{2-} with singlet−triplet splittings of 600[14] and 177 cm^{-1},[45] respectively, demonstrates that low-lying excited states are possible for fullerene anions. However, one would expect rather different excited energy levels for the 1− and 3− anions, which is difficult to reconcile with the observation that, in the same solvent, the temperature-dependent line widths are similar for the two anions (Figures 2 and 7). It is likely that the temperature-dependent line broadening is determined by a characteristic that the two anions have in common.

The line widths for C_{60}^- increase with increasing temperature and then tend to plateau (Figure 2). The maximum line widths and the temperatures at which the plateau in line widths is reached are solvent-dependent. The broadest lines at the plateau and lowest temperature for beginning of the plateau were observed for the K^+ salt dissolved in MeTHF. The narrowest lines and highest temperature for the plateau were observed for the same salt in DMSO. This comparison suggests that counterion is not the dominant factor in determining the limiting line width or the temperature at which the line width plateaus. Intermediate values were observed for electrochemically prepared samples. For these data sets the high concentration of ions from the supporting electrolyte does not appear to correlate with either extreme of line width behavior. The similarity of line widths above about 150 K in 4:1 toluene:acetonitrile and

in 4:1 toluene:DMSO suggests that the polarity of DMSO or specific interaction with DMSO are not dominant factors in determining the line widths.

The temperature at which the line widths tends to plateau increases in the order MeTHF <4:1 toluene:acetonitrile ~4:1 toluene:DMSO <DMSO, which is the order of increasing melting/softening points for the solvents. In higher melting solvents it has been noted that the line widths increase up to the melting point of the solvent.[7,8] The nitroxyl radical tempo was used as a probe of local mobility, which may be quite different from the bulk mobility of the solvent. The temperature range in which the tumbling correlation time for tempo went from $>\sim 10^{-8}$ to $<10^{-11}$ s^{-1} also increased in the order MeTHF <4:1 toluene:acetonitrile <DMSO. These comparisons suggest that the increasing line widths for C_{60}^- are due to increasing mobility of the anion or of molecules around it. Although the viscosity of the solvents change rapidly in the vicinity of the melting/softening temperature, except in DMSO the line widths for C_{60}^- do not change abruptly in this temperature region. The changes in solute and solvent mobility may be more gradual going through the glass transition temperature for the mixed solvents than at the melting point of crystalline DMSO.

Literature values of tumbling correlation times for C_{60} in fluid solution at room temperature include 16 ps in CS_2 [46] and 16.3 ps in toluene.[47] In solid C_{60} the tumbling correlation time has been estimated as 9 ps at 283 K[48] and about a nanosecond at 233 K,[49] which suggests that the tumbling correlation time at room temperature may not change significantly on going from solid to solution and that it is strongly temperature-dependent below room temperature. Although the Stokes−Einstein model relating tumbling correlation time to viscosity appears to work well for neutral C_{60} in fluid solution,[47,50] the similarity in correlation times between solid and solution samples indicates a more complicated behavior when a wider range of environments is considered. In solid salts of C_{60}^- the tumbling correlation time is sufficiently short at room temperature that the solid state ^{13}C NMR spectrum obtained without magic angle spinning is narrow, but broadens as the temperature is decreased due to slowing of the anion rotation.[38,39] This limited data on anion dynamics indicate similarity with the dynamics of the neutral parent. The combined data suggest that there may not be a large change in mobility of C_{60}^- or C_{60}^{3-} at the melting point of a solvent so the lack of abrupt changes in line widths at the melting point of the solvent does not rule out a model in which the line widths are determined by mobility.

In an earlier study it was argued that molecular rotation was not the cause of the line broadening because there was no hyperfine splitting to average.[8] An important point that is made in ref 8 is that the typical case in which molecular motion causes broad EPR lines is when there is incomplete motional averaging of anisotropic hyperfine interaction and that case is not appropriate for C_{60}^-. However, molecular motion can effect line widths via its impact on spin−lattice relaxation if the line widths are relaxation rate determined. Extrapolation of the strong temperature dependence of $1/T_1$ measured by SR for C_{60}^- (Figure 5) and C_{60}^{3-} (Figure 9) at low temperatures gives relaxation rates on the order of those calculated from the temperature-dependent contributions to the line widths. This similarity suggests that the CW line widths above about 70 K are determined by electron spin relaxation.[7,11]

Spin rotation is a relaxation mechanism that is inversely proportional to tumbling correlation time. This contribution to $1/T_1$ is given by $(g - g_e)^2/9\tau_c$,[51] where g_e is the free electron g value. Assuming $g = 1.997$ and $\tau_c = 9$ ps at room temperature, this contribution would only be about 3×10^5 s^{-1}. This is orders of magnitude smaller than the observed values of $1/T_1$ for the C_{60} anions and does not appear to determine the relaxation rate.

Increasing mobility causes an increase in spin−lattice relaxation rates for nitroxyl radicals in glassy solvents between 100 and 150 K.[30] For example, at 100 K $1/T_1$ for tempone was about a factor of 3 larger in decahydronaphthalene than in 1:1 water:glycerol, where the nitroxyl radical is less mobile. Spin−lattice relaxation of the nitroxyl radicals was interpreted in terms of modulation of spin−orbit coupling by molecular vibrations.[30] The model proposed for the C_{60} anions is that increasing motion of the anion and of solvent molecules in the vicinity of the anion results in transfer of energy to vibrational modes that modulate the spin−orbit coupling and thereby increases the rate of electron spin−lattice relaxation. The deviations of the low-temperature g values from $g = 2.002$ are similar for C_{60}^- and C_{60}^{3-}, which suggests that spin−orbit coupling is similar for the two anions. The vibrational structures are expected to be similar for C_{60}^- and C_{60}^{3-} so this model predicts similar behavior for the two anions. The temperature dependence is a function of the Boltzmann populations of the vibrational energy levels and of the translational/rotational motions that transfer energy to the vibrational modes.

The relaxation rates for C_{60}^- and C_{60}^{3-} are faster and more strongly temperature dependent than is observed for typical $S = 1/2$ organic radicals derived from molecules with nondegenerate ground states.[7] Faster relaxation is observed for radicals with degenerate ground states due to spin−orbit interaction.[7,8] However, even compared with other radicals with degenerate ground states the relaxation rates for the C_{60} anions are unusually rapid. Reed et al. have suggested an analogy between C_{60} and a heavy atom.[6] For closely related coordination environments electron spin−lattice relaxation is faster and more strongly temperature dependent for $4d^1$ Mo(V)[33] than for $3d^1$ Cr(V)[32] and for $4d^9$ Ag(II) than for $3d^9$ Cu(II).[52] The faster electron spin relaxation rates for C_{60}^- and C_{60}^{3-} than for other organic radicals derived from molecules with orbitally degenerate ground states may be further examples of the trend toward increased temperature dependence for heavier atoms. Excited states also may be involved.

Solvent Effects. Toluene:acetonitrile (4:1) and DMSO solutions of C_{60} anions were selected to test differences in interaction of the solvents with the anions. Below about 70 K the temperature-dependent electron spin relaxation rates and line widths for C_{60}^- and C_{60}^{3-} in DMSO and 4:1 toluene:acetonitrile exhibit substantial similarities. The preceding paragraphs have shown two major differences between the solvents. (1) As a solvent for EPR spectroscopy, DMSO has the disadvantage that it crystallizes at low temperature rather than forming a glass. Crystallization can cause exclusion of solute from the lattice and concomitant increase in the local concentration of solute. Locally high concentrations of solute may be the reason why anisotropic spectra were not observed for a salt of C_{60}^{3-} dissolved in pure DMSO, but anisotropic spectra were observed for ca. 0.2 mM C_{60}^{3-} in DMSO containing supporting electrolyte. (2) The much higher melting point of DMSO than of 4:1 toluene:acetonitrile results in substantially slower molecular motion and slower electron spin relaxation in DMSO than in 4:1 toluene:acetonitrile. This is suggested as the cause for the narrower lines for C_{60}^- in DMSO than in 4:1 toluene:acetonitrile between 100 and 200 K. These two effects are so large that it is difficult to assess the possible impact of differences in ion pairing that may occur in the two solvents.

Conclusions. There are substantial similarities between the temperature dependence of the EPR line shapes and electron

spin relaxation rates for C_{60}^- and C_{60}^{3-}. At 8 K the axial CW spectrum of C_{60}^- and the rhombic spectrum of C_{60}^{3-} demonstrate distortion from I_h symmetry consistent with substantial Jahn−Teller distortion. Below 70 K the change from DMSO to 4:1 toluene:acetonitrile as solvent has little impact on the CW line shapes or the electron spin relaxation rates. These samples contained 0.1 M electrolyte, which may change the solvent structure sufficiently to reduce the tendency to form locally high concentrations of solute at low temperature. The distribution in values of T_1 and the line shapes in the wings of the CW spectra are consistent with the presence of a distribution of distortions. The decreasing g anisotropy for both anions with increasing temperature up to about 70 K is attributed to dynamic averaging of inequivalent distorted structures. The faster phase memory relaxation rates in the high-field wing of the spectrum of C_{60}^- and in both high- and low-field wings of the spectrum of C_{60}^{3-} support the proposal of a dynamic process. The solvent dependence of the temperature-dependent line widths above about 70 K is attributed to mobility of the solute and solvent molecules.

Acknowledgment is made to the donors of the Petroleum Research Fund, administered by the American Chemical Society, for partial support of this work. An NSF shared instrument grant (CHE-9318714) for purchase of the Bruker ESP380E is gratefully acknowledged. R.K. was an Undergraduate Research Associate at the University of Denver, summer 1994. A.K. was an NSF-supported Research Experience for Undergraduates participant at the University of Denver, summer 1995.

References and Notes

(1) Bochvar, D. A.; Gal'pern, E. G. *Dokl. Akad. Nauk SSSR* **1973**, *209*, 610.

(2) Haddon, R. C.; Brus, L. E.; Raghavachari, K. *Chem. Phys. Lett.* **1986**, *125*, 459.

(3) Haymet, A. D. J. *Chem. Phys. Lett.* **1985**, *122*, 421.

(4) Disch, R. L.; Schulman, J. M. *Chem. Phys. Lett.* **1986**, *125*, 465.

(5) Kondo, H.; Momose, T.; Shida, T. *Chem. Phys. Lett*. **1995**, *237*, 111.

(6) Stinchcombe, J.; Pénicaud, A.; Bhyrappa, P.; Boyd, P. D. W.; Reed, C. A. *J. Am. Chem. Soc*. **1993**, *115*, 5212.

(7) Schell-Sorokin, A. J.; Mehran, F.; Eaton, G. R.; Eaton, S. S.; Viehbeck, A.; O'Toole, T. R.; Brown, C. A. *Chem. Phys. Lett*. **1992**, *195*, 225 and references therein.

(8) Dubois, D.; Jones, M. T.; Kadish, K. M. *J. Am. Chem. Soc*. **1992**, *114*, 6446.

(9) Rataiczak, R. D.; Koh, W.; Subramanian, R.; Jones, M. T.; Kadish, K. M. *Synth. Met*. **1993**, *55*−57, 3137.

(10) Jones, M. T.; Kadish, K. M.; Subramanian, R.; Boulas, P.; Vijayashree, M. N. *Synth. Met*. **1995**, *70*, 1341.

(11) Khaled, M. M.; Carlin, R. T.; Trulove, P. C.; Eaton, G. R.; Eaton, S. S. *J. Am. Chem. Soc*. **1994**, *116*, 3465.

(12) Ruoff, R. S.; Tse, D. S.; Malhotra R.; Lorents, D. C. *J. Phys. Chem.* **1993**, *97*, 3379.

(13) Carlin, R. T.; Trulove, P. C.; Eaton, G. R.; Eaton, S. S. In *Fullerenes: Recent Advances in the Chemistry and Physics of Fullerenes and Related Materials*; Kadish, K. M., Ruoff, R. S., Eds.; The Electrochemical Society: Pennington, NJ, 1994; p 986.

(14) Trulove, P. C.; Carlin, R. T.; Eaton, G. R.; Eaton, S. S. *J. Am. Chem. Soc*. **1995**, *117*, 6265.

(15) Kato, T.; Kodama, T.; Shida, T. *Chem. Phys. Lett*. **1993**, *205*, 405.

(16) Lawson, D. R.; Feldheim, D. L.; Foss, C. A.; Dorhout, P. K.; Elliott, C. M.; Martin, C. R.; Parkinson, B. *J. Electrochem. Soc*. **1992**, *139*, L68.

(17) Quine, R. W.; Eaton, G. R.; Eaton, S. S. *Rev. Sci. Instrum*. **1987**, *58*, 1709.

(18) Quine, R. W.; Eaton, S. S.; Eaton, G. R. *Rev. Sci. Instrum*. **1992**, *63*, 4251.

(19) Provencher, S. W. *Biophys. J*. **1976**, *16*, 27. Provencher, S. W. *J. Chem. Phys*. **1976**, *64*, 2772.

(20) Pénicaud, A.; Hsu, J.; Reed, C. A. *J. Am. Chem. Soc*. **1991**, *113*, 6698.

(21) Salikhov, K. M.; Tsvetkov, Yu. D. In *Time Domain Electron Spin Resonance* Kevan, L., Schwartz, R. N., Eds.; Wiley: New York, 1979; Chapter 7.

(22) Eaton, S. S.; Eaton, G. R. *J. Magn. Reson*. **1993**, *A102*, 354.

(23) Freed, J. H. In Spin Labeling: Theory and Applications, Berliner, L. J., Ed.; Academic Press: New York, 1976; Chapter 3.

(24) Koga, N.; Morokuma, K. *Chem. Phys. Lett*. **1992**, *196*, 191.

(25) Adams, G. B.; Sankey, O. F.; Page, J. B.; O'Keeffe, M. *Chem. Phys*. **1993**, *176*, 61.

(26) Allemand, P.-W.; Srdanov, G.; Koch, A.; Khemani, K.; Wudl, F.; Rubin, Y.; Diederich, F.; Alvarez, M. M.; Anz, S. J.; Whetten, R. L. *J. Am. Chem. Soc*. **1991**, *113*, 2780.

(27) Greaney, M. A.; Gorun, S. M. *J. Phys. Chem*. **1991**, 95, 7142.

(28) Bhyrappa, P.; Paul, P.; Stinchcombe, J.; Boyd, P. D. W.; Reed, C. A. *J. Am. Chem. Soc*. **1993**, *115*, 11004.

(29) Ghim, B. T.; Eaton, S. S.; Eaton, G. R.; Quine, R. W.; Rinard, G. A.; Pfenninger, S. *J. Magn. Reson.* **1995**, *A115*, 230.

(30) Du, J.-L.; Eaton, G. R.; Eaton, S. S. *J. Magn. Reson*. **1995**, *A115*, 213.

(31) Du, J.-L., Eaton, G. R.; Eaton, S. S. *J. Magn. Reson.* **1995**, *A117*, 67.

(32) Konda, R.; Du, J.-L.; Eaton, S. S.; Eaton, G. R. *Appl. Magn. Reson*. **1994**, *7*, 185.

(33) Husted, R.; Du, J.-L.; Eaton, G. R.; Eaton, S. S. *Magn. Reson. Chem*. **1995**, *33*, S66.

(34) Du, J.-L.; Eaton, G. R.; Eaton, S. S. *J. Magn. Reson*. **1995**, *A115*, 236.

(35) Boulas, P.; Kutner, W.; Jones, M. T.; Kadish, K. M. *J. Phys. Chem*. **1994**, *98*, 1282.

(36) Krusic, P. J.; Wasserman, E.; Parkinson, B. A.; Malone, B.; Holler, E. R., Jr. *J. Am. Chem. Soc*. **1991**, *113*, 6274.

(37) Douthwaite, R. E.; Brough, A. R.; Green, M. L. H. *J. Chem. Soc., Chem. Commun*. **1994**, 267.

(38) Chen, J.; Huang, Z.-E.; Cai, R.-F.; Shao, Q.-F.; Chen, S.-M.; Ye, H.-J. *J. Chem. Soc., Chem. Commun.* **1994**, 2177.

(39) Chen, J.; Cai, R.-F.; Huang, Z.-E.; Shao, Q.-F.; Chen, S.-M. *Solid State Commun*. **1995**, *95*, 239.

(40) Jones, M. T.; Kadish, K. M.; Subramanian, R.; Boulas, P.; Vijayashree, *Synth. Met*. **1995**, *70*, 1341.

(41) Moriyama, H.; Kobayashi, H.; Kobayashi, A.; Watanabe, T. *J. Am. Chem. Soc*. **1993**, *115*, 1185.

(42) Pénicaud, A.; Peréz-Benitez, A.; Gleason, R.; Muñoz, E.; Escudero, R. *J. Am. Chem. Soc*. **1993**, *115*, 10392.

(43) Mehran, F.; Schell-Sorokin, A. J.; Brown, C. A. *Phys. Rev. B* **1992**, *46*, 8579.

(44) Bossard, C.; Rigaut, S.; Astruc, D.; Delville, M.-H.; Félix, G.; Février-Bouvier, A.; Amiell, J.; Flandrois, S.; Delhaès *J. Chem. Soc., Chem. Commun*. **1993**, 333.

(45) Boulas, P.; Jones, M. T.; Kadish, K. M.; Ruoff, R. S.; Lorents, D. C.; Tse, D. S. In "*Fullerenes: Recent Advances in the Chemistry and Physics of Fullerenes and Related Materials*"; Kadish, K. M., Ruoff, R. S., Eds.; The Electrochemical Society: Pennington, NJ, 1994; p 995.

(46) Canet, D.; Robert, J. B.; Tekely, P. *Chem. Phys. Lett*. **1993**, *212*, 483.

(47) Jones, J. A.; Rodriguez, A. A. *Chem. Phys. Lett*. **1994**, *230*, 160.

(48) Johnson, R. D.; Yannoni, C. S.; Dorn, H. C.; Salem, J. R.; Bethune, D. S. *Science* **1992**, *255*, 1235.

(49) Yannoni, C. S.; Johnson, R. D.; Meijer, G.; Bethune, D. S.; Salem, J. R. *J. Phys. Chem*. **1991**, *95*, 9.

(50) Steren, C. A.; van Willigen, H.; Dinse, K.-P. *J. Phys. Chem*. **1994**, *98*, 7464.

(51) Atkins, P. W.; Kivelson, D. *J. Chem. Phys*. **1966**, *44*, 169.

(52) Du, J.-L.; Eaton, G. R.; Eaton, S. S. *J. Magn. Reson*., in press.

JP953220L